Electron scattering and transmission through SCALPEL masks

M. M. Mkrtchyan, J. A. Liddle, A. E. Novembre, W. K. Waskiewicz, G. P. Watson, L. R. Harriott, and D. A. Muller
Lucent Technologies, Bell Laboratories, Murray Hill, New Jersey 07974

(Received 29 May 1998; accepted 16 September 1998)

Electron scattering in thin solid films used for the fabrication of masks for electron projection lithography, e.g., SCALPEL®, is investigated. We have developed an analytical model to calculate electron transmission through the mask membrane and image contrast due to different scattering properties of the patterned area and the membrane. The model utilizes cross sections for electron elastic and inelastic scattering on an atom with exponentially screened Coulomb potential of the nucleus derived in the first Born approximation. The variety and controversy of theoretical and empirical adjustments of the screening parameter are briefly analyzed and attributed to the misinterpretation of experimental data ignoring the effects mostly due to plural scattering of electrons and dense packing of atoms in thin solid films. This model frees us from the computational limitations of Monte Carlo simulations and proves to be effective for the straightforward characterization of various alternative materials for SCALPEL mask membrane and scatterer. The model includes the appropriate effects of the projection optics and back-focal plane aperture. [S0734-211X(98)10006-9]

I. INTRODUCTION

In the SCALPEL technique an image is generated utilizing different scattering properties of the patterned layer of the mask and the supporting membrane. High contrast can then be achieved using an aperture in the back-focal plane (BFP) of the first projection lens which filters out the electrons elastically scattered to large angles from the patterned area of the mask.[1] The brightness and contrast of the image generated on the wafer then is a function of the BFP aperture size and the material and thickness of both membrane and scatterer. The calculation of this function is the major goal of this article; it will enable us to analyze the possibilities for SCALPEL mask performance improvement. Note, in the current SCALPEL mask, a 275-Å-thick tungsten scatterer on top of 1500 Å SiN_x membrane is normally used along with 0.5 mrad BFP aperture.[2]

II. SCATTERING AND TRANSMISSION OF ENERGETIC ELECTRONS IN THIN FILMS

Aiming for application to very thin films and 100 keV electrons, initially we assume that incident electrons experience (i) only single scattering event per electron and (ii) a negligible energy loss (less than 25 eV in currently used SCALPEL mask membranes) due to inelastic scattering that does not affect the electron velocity. The decrease $dn(z)$ of the number of unscattered electrons, $n(z)$, at the depth z in a compound material is equal to[3,4]

$$dn(z)/n(z) = -[\Sigma N_i \sigma_{\Sigma i}]dz, \tag{1}$$

where $N_i = \rho N_A / A_i$ is the number of atoms per volume, $\sigma_{\Sigma i} = \sigma_{\text{el } i} + \sigma_{\text{inel } i}$ is the sum of total cross sections of the electron elastic and inelastic scattering on an atom of ith species, ρ is the compound density, A_i is the atomic weight of the ith species of the solid material, and $N_A = 6.02 \times 10^{23}$ g atom^{-1} is Avogadro's number.

Integrating Eq. (1), one finds an exponential decrease of the number of unscattered electrons with increasing depth of the beam penetration, z:

$$n(z) = n_0 \exp(-z/\Lambda_\Sigma), \tag{2}$$

where

$$\Lambda_\Sigma = (\Sigma N_i \cdot \sigma_{\Sigma i})^{-1} \tag{3}$$

is the mean free path of an electron between successive scattering events.

While the energy loss of an inelastically scattered electron in a sample of several mean free path thickness causes a negligible change in σ_Σ and can be ignored, multiple scattering has an increasing impact with increasing sample thickness and collection angle. In the case of film thickness comparable with Λ_Σ and collection angles much smaller than the characteristic screening angle θ_{0i} [Eq. (5)], the multiple scattering effect on σ_Σ appears to be small and can be accounted for by adjusting the screening angle.[5–7] The cross section of electron elastic and inelastic scattering will also change depending on the bonding and packing effects present in solids.[8,9] All of these small effects can be approximately accounted for by choosing the screening parameter that gives the best agreement with the experimental measurements of the contrast and transmission of SCALPEL masks (Sec. V).

A. Elastic scattering of fast electrons in thin films

Elastic scattering of a fast electron is caused by its interaction with the atomic nucleus. Therefore, one could expect that the bonding of atoms in compounds and solids will not significantly affect the cross section of elastic scattering.[3–5] There is theoretical and experimental evidence indicating that these effects are relatively important for small angle scattering only;[8] the change of outer-shell electronic structure due to the bonding and packing changes the screening of the nucleus of individual atoms.[9] The effect of bonding on

the small angle elastic scattering is relatively small. Ionization represents an extreme form of chemical shift; it is shown[8,10] that for atomic numbers $Z>3$, single ionization produces less than a 15% increase in scattered intensity at the small scattering angles θ corresponding to $s=\lambda^{-1}\sin(\theta/2)<0.2$, where λ is the electron wavelength. In the same angular range, for diatomic molecules of H_2, N_2, and O_2, it is experimentally found that there is about 10%–30% *reduction* of elastic scattering cross section.[8,11] An additional decrease of elastic scattering intensity in small angle range (less than several mrad) is expected due to plurality of scattering;[6] accounting for multiple scattering effect is especially important in the interpretation of experimental results obtained for thin solid samples.[12] This indicates that the usage of single atom cross sections for elastic scattering for compounds and solids is justified if one accounts for the solid effects and for plurality of scattering.

The differential cross section of an electron elastically scattered on an atom has been calculated by using various methods. Tabulated cross sections, calculated using the first Born approximation and atomic potentials derived from relativistic Hartree–Fock atomic wave functions, and the results obtained from the partial wave approach are more precise but they are derived at the expense of complicated numerical calculations and do not provide analytical dependencies.

The simplest and commonly used method of the differential cross-section calculation for the electron elastic scattering on an atom is based on the application of the first Born approximation to the quantum mechanical problem and use of an atomic exponential potential $V(r)\propto(Ze^2/r)\exp(-r/R)$ that accounts for the screening of the bare nucleus charge, Ze, by the cloud of electrons.[3–5,13] In Lenz's scattering theory[13] the characteristic screening distance is $R\approx a_H/Z^{1/3}$ (a_H is the Bohr radius). The condition of the first Born approximation applicability, $Ze^2/\hbar v\ll 1$,[3] is satisfied in the case of 100 keV electrons ($Z^{4/3}\ll 70$) scattered on the SCALPEL mask membranes made of low Z materials. Here e and v are the electron charge and velocity correspondingly, $\hbar=h/2\pi$, and h is the Planck constant. A general value $R_g=a_H/(\chi Z^{1/3})$ with a correction factor χ is usually used to take into account the difference between the simplified Wentzel model ($\chi=1$) and more sophisticated models for a free atom (e.g., Thomas–Fermi, Hartree–Slater, Hartree–Fock–Slater, etc.).[3–5] This approach leads to Rutherford differential cross section with screening:[3,4,13–15]

$$d\sigma_{\mathrm{el}\,i}/do=[Z_i(Z_i+1)e^4/(m_0^2\gamma^2\beta^4c^4)]\times[2\sin^2(\theta/2)+\theta_{0i}^2]^{-2}, \tag{4}$$

where the commonly used factor Z_i^2 is replaced by $Z_i(Z_i+1)$ to account for the scattering on atomic electrons,[3,14–17] θ_{0i} is the characteristic screening angle of the ith species:[3,4]

$$\theta_{0i}=\chi\lambda/(2\pi R), \tag{5}$$

$\lambda=(h/m_0c\beta\gamma)$ is the electron wavelength, m_0 is the electron rest mass, c is the light velocity in free space, $\beta=v/c=[(E/E_0+1)^2-1]^{1/2}/(E/E_0+1)$, $E_0=m_0c^2=511$ keV, $\gamma=(1-\beta^2)^{-1/2}$, and E is the electron energy. Note, Rutherford cross section with screening deviates essentially from Mott cross section, which accounts for the electron spin effects, in the case of heavy atoms, $Z>40$, and extremely large collection angles ($\theta>10°$) compared to BFP aperture.[4]

The total elastic scattering cross section is obtained by integrating Eq. (4) over the full solid angle:[3,14,15]

$$\sigma_{\mathrm{el}\,i}=2\pi\int_0^{\pi}(d\sigma_i/do)\sin\theta\,d\theta=[4\pi Z_i(Z_i+1)e^4/(m_0^2\gamma^2\beta^4c^4)][\theta_{0i}^2(2+\theta_{0i}^2]^{-1}. \tag{6}$$

For light atoms, the characteristic screening angle $\theta_{0i}=0.011\chi Z^{1/3}$ has a small value and $\sigma_{\mathrm{el}\,i}$ is proportional to θ_{0i}^{-2}:

$$\sigma_{\mathrm{el}\,i}\approx 4\pi Z_i(Z_i+1)e^4/(m_0\theta_{0i}\gamma\beta^2c^2)^2\approx 1.87\times10^{-20}Z_i^{1/3}(Z_i+1)/(\chi\beta)^2. \tag{7}$$

There is a large number of theoretical[3,14–20] and empirical[4,21,22] attempts of adjusting the screening angle on the basis of different suggestions and criterions. Different values, sometimes controversial, were found for the parameter θ_{0i} by different authors.[3,4,14–22] All adjustments can be grouped in two categories based on a straightforward matching of Rutherford cross section given by Eq. (6), (i) with elastic cross sections obtained from more realistic and sophisticated atomic models leading to the values in the range $0.7<\chi<1$, and (ii) with experimental cross sections obtained mostly on solid films leading to the values $1<\chi<2$. Note that $\sigma_{\mathrm{el}}\propto\chi^{-2}$ [Eq. (7)], therefore, the variation of χ in the range 0.7–2 would cause a change of σ_{el} of almost an order of magnitude. Our analysis shows that the large values of $\chi>1.5$ are found as a result of ignoring[21] or underestimating[22] electron inelastic and multiple scattering contributions present in the experiments and, therefore, they must be discarded from further discussion. A semiempirical expression,[4,8]

$$\sigma_{\mathrm{el\,emp}}=1.5\times10^{-20}Z^{3/2}\cdot\beta^{-2}[1-0.23Z/(137\beta)]\ \ (\mathrm{cm}^2), \tag{8}$$

that gives the observed Z dependency for the elastic total cross section for $Z/(137\beta)<1.2$, would be predicted if $\chi\approx0.99$, 0.96, 0.891, 0.832, and 0.776 for the atoms Be, C, Si, Ge, and Au, respectively.[23] This indicates that the widely used Lenz's cross section[4,13] [Eq. (7) with $\chi=1$] gives the least cross section for the electron elastic scattering on an isolated atom.[8] It also shows that screening angle adjustment cannot be done independently of the atomic number.[22] Nevertheless, a value of $\chi\approx1.265$ is commonly used by different authors[14,20] which can be considered as an apparent compromise between controversial results and an attempt of an indirect account for the bonding effects in solids, if one recalls the scattering intensity reduction due to bonding effects[8,11] mentioned above. The results of our measurements of SCALPEL masks contrast and transmission in a SCALPEL proof of lithography (SPOL) tool demonstrate that the best match with the results calculated using Eq. (7) can be found

when χ changes from ≈ 1.175 for light materials to 1.27 for heavy materials. This corresponds to a decrease of the effective cross section of electron elastic scattering on an atom in solids which can be attributed to the combined effect of the adjustments for atomic potential, for plurality of scattering events, and for bonding effects in solid samples. In crystalline solids, the angular dependence of elastic scattering is altered by both Bragg reflection from atomic planes (dramatically) and phonon scattering (perceptible only for heavy materials due to $Z^{3/2}$ dependency).[5] Therefore, the usage of an atomic model is justified only for amorphous solids when both effects are weak.[5]

B. Inelastic scattering of electrons in thin films

The initial direction of an electron incident on the mask membrane is changed not only because of elastic scattering on the nucleus (pure momentum change without the change of kinetic energy), but also because of the transfer of the energy to the medium through various inelastic interactions. Therefore, the total cross section $\sigma_\Sigma = \sigma_{\rm el} + \sigma_{\rm inel}$ has to be used to define the effective mean free path between successive scattering events.[4,13,15,17] Inelastic scattering of a fast electron on an isolated atom is concentrated within much smaller angles than elastic scattering; the corresponding characteristic angle, $\theta_E = [(E+E_0)/(E+2E_0)](\Delta E/E) = \Delta E/(E_0 \gamma \beta^2)$ (ΔE is the energy transferred to an electron of the atom),[4] responsible for the decrease of $d\sigma_{\rm inel}/do$ with increasing of θ, is about ten times smaller than θ_{0i}. The differential cross section $d\sigma_{{\rm inel}\,i}/do$ increases with the decrease of θ and gets larger than $d\sigma_{{\rm el}\,i}/do$ for the angles $\theta < \theta_E$ where $d\sigma_{{\rm el}\,i}/do \propto \theta_{0i}^{-2}$ and does not depend on θ. The ratio $\nu = \sigma_{\rm inel}/\sigma_{\rm el}$ approximately follows the empirical law,[4,5] $\nu = 18/Z$, which demonstrates that for light materials contribution of the inelastic scattering to the total cross section dominates over its elastic counterpart.

Though concentrated within a narrow angular range, the inelastic scattering (in the case of light atoms) will have a significant impact on the effective mean free path of an electron defined as follows:

$$1/\Lambda_\Sigma(\alpha_0) = N_A \rho \Sigma [\sigma_{{\rm el}\,i}(\alpha_0) + \sigma_{{\rm inel}\,i}(\alpha_0)]/A_i = \Sigma [\Lambda_{{\rm el}0\,i} \Phi_{\Sigma - i}(\alpha_0)]^{-1}, \quad (9)$$

where $\Lambda_{{\rm el}0\text{-}i} = [N_i \sigma_{{\rm el}\text{-}i}(0)]^{-1}$ is the mean free path for an electron elastically scattered on ith species, $\sigma_{{\rm el}\text{-}i}(\alpha_0)$ and $\sigma_{{\rm inel}\text{-}i}(\alpha_0)$ are the partial cross sections characterizing the scattering of electrons outside of the back-focal aperture angular range $0 < \theta < \alpha_0$ (see Sec. III). The smaller α_0 and the lighter the atom, the larger the impact of inelastic scattering. Here we have introduced the function

$$\Phi_{\Sigma - i}(\alpha_0) = \alpha_{{\rm el}\,i}(0)[\sigma_{{\rm el}\,i}(\alpha_0) + \sigma_{{\rm inel}\,i}(\alpha_0)]^{-1} = [1 + \nu_i(\alpha_0)]^{-1} \quad (10)$$

which accounts for the change of the mean free path due to electron inelastic scattering.

Assuming a constant energy loss for an electron, $\Delta E = J/2$, where $J \approx 13.5Z$ is the mean ionization energy of the atom, for $\Phi_\Sigma(\alpha_0)$, Lenz[13] has found a formula [Ref. 4, Eqs. (6) and (7)] which is used to calculate the effective contrast thickness in transmission electron microscopy.[4] Lenz's expression for $\Phi_\Sigma(\alpha_0)$ has a singularity at $\alpha_0 = 0$ and does not adequately describe the inelastic scattering distribution for extremely small angular apertures. This singularity is the result of the constant energy loss assumption. It can be avoided by using the entire spectrum of energy loss rather than a discrete loss.[4] Here we calculate $\Phi_\Sigma(\alpha_0)$ using a semiempirical approximation to the inelastic scattering angular distribution applicable to light atoms and to carbon-like compounds (most organic materials); this was done by approximating the empirical energy loss function by a Lorentzian expression in the dielectric theory of plasmon losses in solids.[24] The functions $\Phi_\Sigma(\alpha_0) = \Lambda_\Sigma(\alpha_0)/\Lambda_0$, corresponding to this approach, and $\Phi_{\rm el}(\alpha_0) = \Lambda_{\rm el}(\alpha_0)/\Lambda_0$ [$\Lambda_0 = \Lambda_{\rm el}(0)$] are shown in Fig. 1. These plots demonstrate that inelastic scattering is concentrated within much smaller angles than elastic scattering, $\theta < \theta_{\max} = (2\theta_E)^{1/2}$ where $\theta_E = \beta^{-2}\Delta E/(E + m_0 c^2)$ is the cut off angle[5,24] corresponding to the most probable energy loss; this distribution falls as $(\theta^2 + \theta_E^2)^{-1}$ for $\theta > \theta_E$. For instance, when $\Delta E \approx 20$ eV (comparable with the characteristic plasmon or outer-shell ionization losses in light solid materials), $\theta_E \approx 0.12$ mrad, and 97% of the inelastic scattering is found with scattering angles less than $\theta_{\max} = (2\theta_E)^{1/2} \approx 15$ mrad.[24]

III. ACCOUNT FOR FINITE APERTURE SIZE

Transmission through a SCALPEL mask is defined by the unscattered fraction of electrons in the first approximation only when BFP aperture finite size is ignored.[1] In reality, all electrons scattered in a cone with the apex semiangle $\alpha_0 = \arctan(r_{\rm ap}/f_1)$, where $r_{\rm ap}$ is the back focal plane aperture radius and f_1 is the focal length of the first projection lens (for details see Ref. 1), contribute to the transmission. It is natural to assume that the effect of aperture size is described by the partial cross section of the scattering:[4,5]

$$\sigma_i(\alpha_0) = 2\pi \int_{\alpha_0}^{\pi} (d\sigma_i/do) \sin\theta \, d\theta. \quad (11)$$

A comprehensive account for the limited angular aperture can be done using Everhart's single-scattering (ESS) model.[25] We denote $n_{\alpha 0}(z)$ the number of electrons elastically scattered from the depth z inside the cone with the apex semiangle α_0. The decrease of $n_{\alpha 0}(z)$ due to electron scattering in the layer z, $z + dz$ is described then as follows:

$$dn_{\alpha 0}(\xi) = -0.5\kappa n_{\alpha 0}(\xi) d\xi/(1-\xi)\varphi(\alpha_0, \alpha_i). \quad (12)$$

Here $\xi = z/R_{\rm ful}$, $R_{\rm ful}$ is the electron full range in the material, $\kappa = 0.024Z^2/A$ is the parameter of the ESS theory, and $\varphi(\alpha_0, \alpha_i)$ is a function which characterizes the number of electrons elastically scattered outside of the aperture cone:

$$\varphi(\alpha_0,\alpha_i)=\int_{\alpha_0}^{\pi}(\sin^2\ \theta/2+\theta_{0i}^2)^{-2}\ \sin\ \theta\ d\theta$$
$$=[(1+\theta_{0i}^2)(\sin^2\ \alpha_0/2+\theta_{0i}^2)]^{-1}(1-\sin^2\ \alpha_0/2). \tag{13}$$

Integrating Eq. (12) from $z=0$ to $z=t_m$ one can get the following expression for the fraction of electrons transmitted through the membrane of thickness t_m:

$$T(\alpha_0)=n_{\alpha 0}(\xi_m)/n_{\alpha 0}(0)=(1-\xi_m)^{\kappa\varphi(\alpha 0,\alpha i)},$$
$$\xi_m=t_m/R. \tag{14}$$

For thin films of interest, $\xi_m \ll 1$, Eq. (14) can be expanded in a series. In the approximation $O(\xi_m^2)$ it represents an exponential function

$$T(\alpha_0)=\exp[-z/\Lambda_{\rm el}(\alpha_0)], \tag{15}$$

which is reminiscent of Eq. (3) but with electron mean free path as a function of the aperture size:

$$\Lambda_{\rm el}(\alpha_0)=\Lambda_{\rm el0}\Phi_{\rm el}(\alpha_0). \tag{16}$$

Here

$$\Lambda_{\rm el0}\equiv\Lambda_{\rm el}(0)=(\Sigma\sigma_{{\rm el}\text{-}i}N_A\rho/A_i)$$

and

$$\Phi_{\rm el}(\alpha_0)=(\rho R_{\rm ful}C_T/c^4\beta^4\gamma^2)$$
$$\times(\sin^2\ \alpha_0/2+\theta_{0i}^2)/[\theta_{0i}^2(1-\sin^2\ \alpha_0/2)] \tag{17}$$

is a function that characterizes the aperture size influence on the mean free path of electron scattering. Using the Thomson–Whiddington empirical equation[3,25] for the electron range, $R_{\rm ful}C_T\approx\gamma^2c^4\beta^4/\rho$, we find for the function $\Phi_{\rm el}(\alpha_0)$ an expression which is totally defined by two parameters, by the aperture size, α_0, and by the characteristic screening angle, θ_{0i}:

$$\Phi_{\rm el}(\alpha_0)=(\sin^2\ \alpha_0/2+\theta_{0i}^2)/[\theta_{0i}^2(1-\sin^2\ \alpha_0/2)]. \tag{18}$$

One can see that for extremely small apertures, $\alpha_0 \ll \theta_{0i}$, $\Phi_{\rm el}(\alpha_0)\to 1$ independent of the membrane material, while for $\alpha_0 \geqslant \theta_{0i}$, $\Phi_{\rm el}(\alpha_0)$ depends on the membrane material [Fig. 1(b)]. Note that the usage of the partial elastic cross section [Eq. (11)] gives for the function $\Phi_{\rm el}(\alpha_0)=\Lambda_{\rm el}(\alpha_0)/\Lambda_{\rm el0}$ exactly the same result as ESS theory does [Fig. 1(a)] indicating that the partial cross section is appropriate for thin films only when single scattering dominates over multiple counterpart. For a SCALPEL system and SiN_x mask membrane ($\alpha_0=0.5$ mrad, $\theta_{0i}\approx 27$ mrad) the function $\Phi_{\rm el}(\alpha_0)\approx 1.0$ which indicates that in this case the account for a finite aperture has a negligible effect on the electron effective mean free path between the elastic scattering events. Therefore, for small α_0, in a model that accounts for *only elastic scattering*, the transmission of electrons through the SCALPEL mask membrane can be calculated assuming that any electron, elastically scattered in a thin membrane, will be stopped by the BFP aperture.[1] Aperture finite size will affect the results for relatively large α_0 (larger than the characteristic screening angle θ_{0i}).

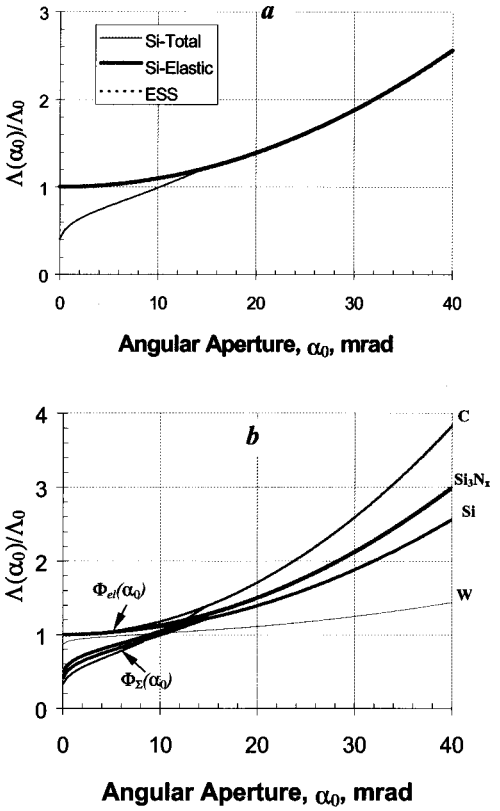

FIG. 1. Functions $\Phi_{\rm el}(\alpha_0)=\Lambda_{\rm el}(\alpha_0)/\Lambda_{\rm el0}$ and $\Phi_\Sigma(\alpha_0)=\Lambda_\Sigma(\alpha_0)/\Lambda_{\rm el0}$ calculated for 100 keV electrons scattered in different materials. The dotted curve (a), obtained from single-scattering model for Si ($\theta_{0i}=27$ mrad) exactly matches with the one obtained using Eq. (11) for the partial elastic cross section: $\Lambda_{\rm el0}=\Lambda_{\rm el}(0)$.

The finite size of the BFP aperture will apparently have noticeable impact on the results if small-angle inelastic scattering dominates over elastic scattering, e.g., in the case of light atoms (see Sec. II). This is demonstrated by the plots for the function $\Phi_\Sigma(\alpha_0)=\Lambda_\Sigma(\alpha_0)/\Lambda_{\Sigma 0}$ in Fig. 1. These plots also show that in the case of relatively large apertures, $\alpha_0>10$ mrad, one can neglect (for all atoms considered) the impact of inelastic scattering on the electron mean free path, and, therefore, on the membrane transmission related to $\Lambda_\Sigma(\alpha_0)$:

$$T(\alpha_0)=n(t_{\rm mem})/n_0=\exp(-t_{\rm mem}/\Lambda_\Sigma). \tag{19}$$

From Fig. 1(b) one can see that the lighter the atom the larger the effect of the inelastic scattering. The impact of inelastic scattering on $\Lambda_\Sigma(\alpha_0)$ [and, therefore, on the membrane transmission defined by Eq. (19)] is significant for angular apertures much smaller than the characteristic screening angle, especially for light atoms. The ratio $\Lambda_\Sigma(\alpha_0)/\Lambda_{\Sigma 0}$, calculated for different compounds of C, Si, Al, namely for SiO_2, SiC, Si_3N_4, and Al_2O_3 [not shown in Fig. 1(b)], is very close to the one shown for Si_3N_4 which is between the values obtained for C and Si.

TABLE I. Physical parameters, electron scattering cross sections, σ, and mean free paths, Λ, for different materials: ρ is in g/cm^3, σ is in 10^{-20} cm^2, and Λ in nm units.

	A	Z	ρ,	$\sigma_{\text{el-emp}}$	$\sigma_{\text{el-Lenz}}$	$\sigma_{\text{el-cor}}$[a]	$\sigma_{\text{el-emp}}$	$\Lambda_{\text{el-Lenz}}$	$\Lambda_{\text{el-cor}}$	$\Lambda_{\text{eff}}(0)$	$\Lambda_{\text{eff}}(0.5)$
Be	9.012	4	1.86	39	39.6	35.8	92.8	203	225	62.6	81.4
C[b]	12.01	6	2.0	72	68.1	57.4	118	150	178	58.34	74.4
Graphite	12.01	6	2.27	72	68.1	57.4	101.5	129	153	55.4	69.7
Diamond	12.01	6	3.52	72	68.1	57.4	65.4	83.4	99	46.2	55.7
Si_3N_4	20.00	10	3.44	153	134	106	111.3	71.8	91	44.5	53.2
SiO_2[c]	20.0	10	2.65	153	134	106	144.5	93.2	118	50.1	61.4
SiC	20.0	10	3.22	153	134	106	119	76.8	97.5	46	55.3
Al_2O_3	20.4	10	3.97	153	134	106	98.5	63.6	80.7	41.8	49.5
Al	26.98	13	2.7	225	191	144	191.3	87	115	49.5	60.5
Si	28.08	14	2.33	250	211	158	230.8	95.1	126	51.4	63.5
Cr	51.99	24	7.19	544	432	298	138.5	27.8	40.3	27.5	30.6
$TaSi_2$	79.04	34	9.14	886	687	459	165.6	20.9	31.3	23	25
Ge	72.59	32	5.32	815	634	428	261	35.7	52.8	32.8	37.4
W	183.8	74	16.6	2457	1938	1240	182	8.14	12.7	11.1	11.5
Pt	195.1	78	21.5	2617	2079	1313	174	7.26	11.5	10.2	10.6

[a]Calculated from Eq. (7) using a correction factor χ that weakly depends on Z increasing from 1.175 for light materials to 1.27 for heavy atoms.
[b]Amorphous carbon.
[c]Quartz.

IV. CONTRAST OF A SCALPEL MASK

The pattern in a SCALPEL mask is usually formed by etching Tungsten films (about 30 nm thick) deposited on top of a SiN_x membrane (about 150 nm thick) supported by a massive Si grillage.[1] The function of the heavy metal film is to scatter the incident beam electrons to angles large enough to be stopped by the back-focal plane aperture.[1] The contrast of a SCALPEL mask with a single-layer scatterer on top of a membrane is simply defined by the equation[1,26]

$$C = 1 - T_{\text{scat}} = 1 - \exp(-t_{\text{scat}}/\Lambda_{\text{scat}}), \tag{20}$$

which represents the difference of electron transmissions through the membrane, T_{mem} [Eq. (19)], and through the double layer (scatterer plus membrane), $T_{\text{scat}}T_{\text{mem}}$, normalized to T_{mem}. In further discussions, we will use the following notations: $\Lambda_{\text{mem}} \equiv \Lambda_{\text{mem}\Sigma}(\alpha_0)$ and $\Lambda_{\text{scat}} \equiv \Lambda_{\text{scat}\Sigma}(\alpha_0)$ for the effective mean free path of electrons in the film and in the scatterer, respectively; t_{mem} and t_{scat} for the thickness of the membrane and the scatterer correspondingly. According to Eq. (20), the contrast is solely defined by the scatterer material and thickness and does not depend on the supporting membrane characteristics. To calculate the contrast for a mask with a multilayer scatterer, it is necessary to make the following replacement:

$$t_{\text{scat}}/\Lambda_{\text{scat}} = t_{\text{scat-1}}/\Lambda_{\text{scat-1}} + t_{\text{scat-2}}/\Lambda_{\text{scat-2}} + \cdots, \tag{21}$$

where $t_{\text{scat-}j}$ is the thickness of the jth layer and $\Lambda_{\text{scat-}j}$ is the electron effective mean free path in the jth layer.

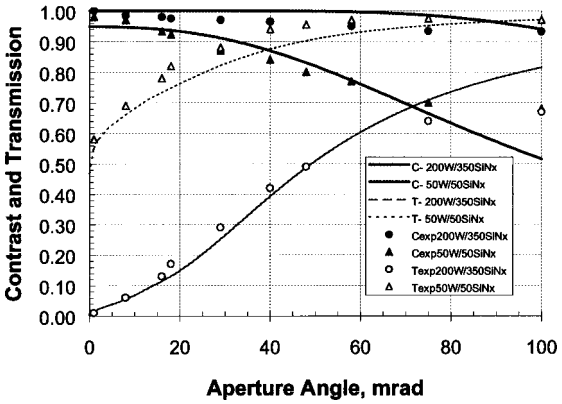

FIG. 2. Experimental and calculated results for contrast and transmission as a function of back focal plane aperture size for two different membrane (Si_3N_4) plus scatterer (W) masks. Symbols represent TEM measurement results: (Ref. 1) circles—$t_{\text{mem}} = 350$ nm, $t_{\text{scat}} = 200$ nm; triangles—$t_{\text{mem}} = 50$ nm, $t_{\text{scat}} = 50$ nm. Accelerating voltage is equal to 120 kV.

V. RESULTS AND CONCLUSION

The electron scattering characteristics for different materials calculated for the case $E = 100$ keV using different approaches are summarized in Table I. Note that the corrected total cross section of elastic scattering is smaller than the results predicted by the empirical or the Lenz's formula. This noticeable difference is the result of the combined effect of adjustment for atomic potential, for plurality of scattering events, and for densely packed atoms on real solid samples. The correction factor χ is chosen to get the best match of calculated transmission coefficient, T, and contrast, C, with our TEM[1] (Fig. 2) and SPOL measurement results (Table II).

In Fig. 2 the dependence of the contrast and transmission of SCALPEL mask is displayed as a function of BFP aperture size for two different membrane/scatterer combinations. One can see that the inelastic scattering effect is localized in a very narrow range of small angles which is less than the convergence angle of a TEM beam (about 1 mrad) used in the experiment.[1] The deviation of calculated results from the experiment gets larger for thicker samples and relatively large apertures, apparently, due to the increase of multiple scattering effect.[23] Nevertheless, the results presented in Fig. 2 show that the single-collision based simple model with empirically corrected cross sections demonstrates the capa-

TABLE II. Comparison of calculated and measured results for C and T for two masks with identical targeted thicknesses fabricated at different time.

			Measured		Simulated	
Mask layer	Material	Thickness (nm)	C(%)	T(%)	C(%)	T(%)
Scatterer	W	27.5	90.6 91.8	4.12 4.15	91	4.96[a]
Membrane	SiN_x	150				
	Cr	6				

[a]Calculated T is always larger than the measured value apparently due to the effect of ''shadowing'' of the transmitted electrons by the massive Si struts of grillage not accounted for in the model.

bility to describe the electron scattering in membrane plus scatterer type of targets for a relatively wide range of aperture size change.

Using electron mean free paths in different materials (the last column in Table I), the values for T and C were calculated from Eqs. (19) and (20) for a SCALPEL mask with different membrane and scatterer materials and their combinations. The results are shown in Fig. 3. The plots presented in Fig. 3(a) show that the transmission variation for membranes of given thickness made of different light atoms and their compounds is relatively small. This indicates that the electron transmission is insensitive to even large changes in the concentration of the individual components. For instance, any change in the concentration of Si in the membrane made of its compounds (Si_2N_4, SiC, SiO_2) to increase membrane conductivity will not affect the membrane transparency noticeably. Si_2N_4, SiC, and diamond films provide the least transmission. Silicon and quartz demonstrate moderate transparency to 100 keV electrons. As one could expect, a carbon membrane provides the highest electron transmission. For instance, the electron transparency of a carbon membrane of 1000 Å thickness is about 60% higher than the transparency of a silicon nitride film of the same thickness (equal to 15%). From Fig. 3(a) it is also seen, that up to 50 Å thickness, any residual Cr layer on top of a membrane will decrease its transparency not more than 13%.

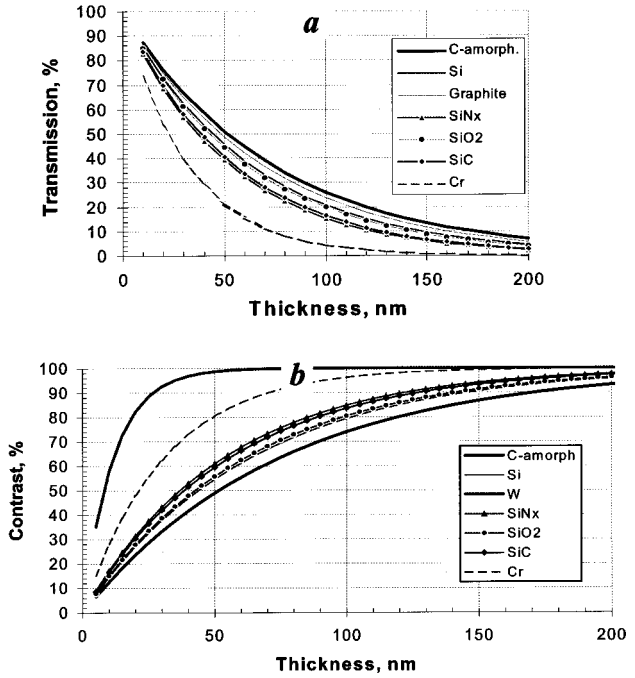

FIG. 3. Transmission of 100 keV electrons through different membranes (a) and contrast from different scatterers (b) as a function of the membrane or scatterer thickness: Angular aperture $\alpha_0 = 0.5$ mrad.

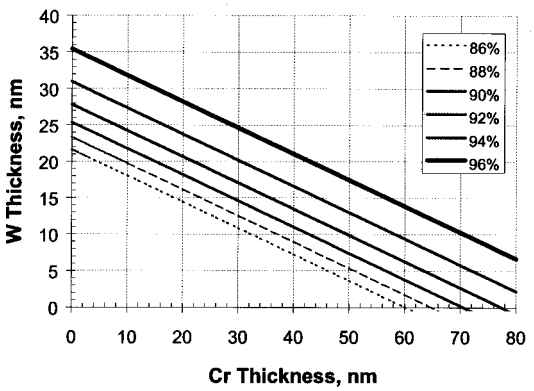

FIG. 4. Constant levels of contrast rendered by W–Cr bilayer scatterer. The slopes of the lines are defined by the ratio of the electron mean free paths in individual scattering layers, Λ_W/Λ_{Cr}.

Figure 3(b) displays the contrast calculated for different scatterers as a function of the film thickness. The plots corresponding to the light atoms and their compounds show that they are ineffective scatterers compared to high Z materials. Nevertheless, over 90% contrast, in principle, can be achieved with Si_2N_4, SiC, SiO_2, or Si films as thick as 1500 Å. Several issues related to the scatterer thickness increase, such as deposition and etching of thick films, formation of high aspect ratio features with vertical walls, electron energy losses and related mask heating, energy spread of electrons scattered into the back focal aperture, etc., has to be addressed in order to understand the feasibility of using light compounds as scatterers for the SCALPEL mask.

The scatterer thickness can be reduced by using bilayers consisting of light and heavy atoms and their compounds used in the semiconductor processing (e.g., Cr, W, $TaSi_2$, etc.). Another advantage of the usage of bilayer scatterers is the possibility of stress reduction by an appropriate combination of scattering layers thicknesses and materials. Figure 4 is an example displaying the relationship between the thickness of the major, W, and the thickness of an additional, Cr, scattering layer that provides a desired level of contrast. The slopes of the lines are defined by the ratio of the electron mean free paths in the individual scattering layers, Λ_W/Λ_{Cr}.

ACKNOWLEDGMENTS

The work was partially supported by DARPA under Contract No. MDA972-95-C-0013 and by SEMATECH.

[1]J. A. Liddle, H. A. Huggins, S. D. Berger, J. M. Gibson, G. Weber, R. Kola, and C. W. Jurgensen, J. Vac. Sci. Technol. B **9**, 3000 (1991).

[2]R. A. Farrow, A. E. Novembre, M. L. Peabody, R. Kasica, M. Blakey, J. A. Liddle, K. S. Werder, R. Demarco, L. Ocola, L. Rutberg, T. Saunders, M. Smith, J. Unruh, and F. Qian, J. Vac. Sci. Technol. B (these proceedings).
[3]K. A. Valiev, *The Physics of Submicron Lithography* (Plenum, New York, 1992).
[4]L. Reimer, *Transmission Electron Microscopy, Physics of Image Formation, and Microanalysis* (Springer, Berlin, 1989).
[5]R. F. Egerton, *Electron Energy-Loss Spectroscopy in The Electron Microscopy* (Plenum, New York, 1996).
[6]K. Wong and R. F. Egerton, J. Microsc. **158**, 198 (1995).
[7]G. H. Smith and R. E. Burge, Proc. Phys. Soc. London **81**, 612 (1963).
[8]J. P. Langmore, J. Wall, and M. Isaacson, Optik (Stuttgart) **38**, 335 (1973).
[9]H. Z. Fleishmann, Z. Naturforsch. A **15**, 1090 (1960).
[10]D. T. Cromer and J. T. Waber, Acta Crystallogr. **18**, 104 (1965).
[11]M. Fink and J. Kessler, J. Chem. Phys. **47**, 1780 (1967).
[12]J. S. Halliday, Br. J. Appl. Phys. **11**, 259 (1960).
[13]F. Lenz, Z. Naturforsch. Teil A **9**, 185 (1954).
[14]R. J. Hawryluk, A. M. Hawryluk, and H. I. Smith, J. Appl. Phys. **45**, 2551 (1974).
[15]H. S. W. Massey, Adv. Opt. Electron. Microsc. **4**, 2 (1952).
[16]H. A. Bethe, Phys. Rev. **89**, 1256 (1953).
[17]W. T. Scott, Rev. Mod. Phys. **35**, 231 (1963).
[18]K. Murata, D. Kyser, and C. Ting, J. Appl. Phys. **52**, 4396 (1981).
[19]G. Moliere, Z. Naturforsch. A **2**, 133 (1947); **3**, 78 (1948).
[20]K. Murata, T. Matsukawa, and R. Shimizu, Jpn. J. Appl. Phys. **10**, 678 (1971).
[21]B. P. Nigam, M. K. Sundaresan, and Ta-Wu, Phys. Rev. **115**, 491 (1959).
[22]L. Reimer and K. H. Sommer, Z. Naturforsch. **239**, 1569 (1963).
[23]R. E. Burge and G. H. Smith, Proc. Phys. Soc. London **79**, 672 (1962).
[24]J. Wall, M. Isaacson, and J. P. Langmore, Optik (Stuttgart) **39**, 359 (1974).
[25]T. E. Everhart, J. Appl. Phys. **31**, 1483 (1960).
[26]P. D. Miller, J. M. Gibson, A. J. Bleeker, and J. A. Liddle, J. Vac. Sci. Technol. B **11**, 2352 (1994).